

# The Effect of Plastic Bending on the Electrical Properties of Indium Antimonide

## Part 1 *An Initial Experimental Survey*

R. L. BELL\*, R. LATKOWSKI, A. F. W. WILLOUGHBY\*  
*Metallurgy Department, Imperial College, London, SW 7, UK*

*Received 11 October 1965*

High temperature plastic bending was used to introduce, into indium antimonide single crystals, an excess of dislocations having either In-atoms at the edge of their extra half-planes ("In-dislocations"), or having Sb-atoms there ("Sb-dislocations"). The densities of these two kinds of dislocations were estimated by etch pit techniques. Hall coefficient and electrical conductivity measurements, made on bent samples, indicated that both In- and Sb-dislocations act as acceptor centres in n-type material, and that In-dislocations act as acceptor centres in p-type material. The results are discussed in relation to the theories of Read [22] and Broudy [4].

### 1. Introduction

The study of dislocations in semiconductors is of interest for two reasons. On the one hand the important electrical properties are much more sensitive to the dislocation content than is the case in metals, and thus it is important to know the extent to which the dislocations limit these properties. Conversely, a study of the electrical effects makes available more detailed information on the structure of the dislocations. Semiconductors, such as germanium, silicon, and indium antimonide, are brittle at room temperature, but become plastic at approximately  $0.5 T_m$ , where  $T_m$  is the melting temperature in degrees absolute. The onset of ductility is extremely sensitive to the applied straining rate, dislocation density, impurity content, etc. For indium antimonide, temperatures greater than  $200^\circ\text{C}$  must be achieved before dislocations have appreciable mobility. An advantage of this is that, following the introduction of a definite plastic strain at high temperature, a specimen may be handled easily at room temperature without introducing further dislocations accidentally. A disadvantage is that, at the deformation temperature, some impurities, to which the electrical properties are also very sensitive, may be picked up and diffuse in rapidly. It is un-

fortunate too that, at the temperatures required for plastic deformation, these semiconductors contain such a high density of intrinsic carriers that the electrical effects of dislocations are not detectable.

The effects of dislocations on the room- and low-temperature electrical properties of germanium and silicon have been studied extensively (see, for example, reviews by Haasen and Seeger [1]; Bardsley [2]; van Bueren [3]; Broudy [4]). In these diamond-structure materials, dislocations of opposite sign are equivalent and the choice of sign convention is purely arbitrary. This is not the case in the sphalerite structure in which indium antimonide crystallises, where opposite sign dislocations might have quite different core structures and properties [5-7]. For example, the two opposite sign slip dislocations shown in fig. 1 have In and Sb atoms, respectively, along the edge of their extra half-planes. These will be referred to as "In-" and "Sb-dislocations". Duga [8], Gatos *et al* [9], and Broudy [4] have observed the introduction of acceptor centres due to plastic deformation, whilst Mueller and Jacobsen [10] have found both acceptor and donor action near small-angle boundaries. The acceptor centres introduced by plastic deformation have been ascribed

\*Now in the Engineering Laboratories, University of Southampton.

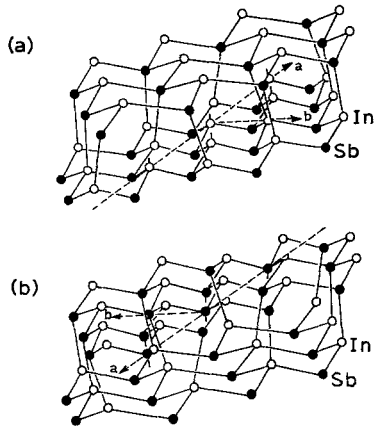


Figure 1 Pure edge dislocations in InSb: (a) In-type; (b) Sb-type.

either to point defects or to In-dislocations. In one bent sample Gatos *et al* [9] found a donor action which they attributed to Sb-dislocations. Holt [6] has argued that In- and Sb-dislocations should both produce acceptor centres. To re-examine this and other features of the problem, pairs of specimens, both n- and p-type, were plastically bent so as to introduce an excess of the one or the other kind of dislocation. Etching experiments were performed to determine the number of each kind of dislocation, and Hall coefficient and electrical conductivity measurements were made both at room temperature and liquid-nitrogen temperature.

## 2. Experimental Procedure

Single crystals grown by the Czochralski [11] technique were supplied by the Royal Radar Establishment, Malvern. The initial carrier concentration of the n-type material was  $N_d - N_a = 4.4 \times 10^{13} \text{ cm}^{-3}$ , and of the p-type material  $N_a - N_d = 6.3 \times 10^{14} \text{ cm}^{-3}$ ; dislocation densities in the as-grown crystals were of order  $10^3 \text{ cm}^{-2}$  or less. To obtain slip on only one of the  $\{111\} \langle 110 \rangle$  systems during the plastic bending experiments, wafers  $2.0 \times 0.9 \times 0.18 \text{ cm}$  were prepared with a slip plane and a slip direction at  $45^\circ$  to the neutral axis, as shown in fig. 2. Adjacent slices from the original crystal were used to make pairs of identical samples which were bent to equal but opposite curvature. Slices, from either side of those from which the pair was made, were used to prepare "control" samples in the shape of bars  $1.5 \times 0.2 \times 0.15 \text{ cm}$ . The surface damage left by cutting operations was removed by etching the specimens in a 1:1 HF:HNO<sub>3</sub> solution.

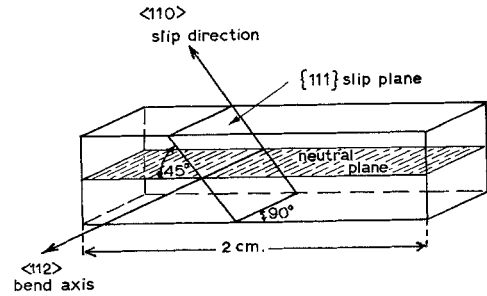


Figure 2 Orientation of specimens for plastic bending.

A preliminary series of experiments had shown that the most uniformly distributed dislocation arrays were obtained when bending was carried out at a very slow rate and at a relatively high temperature, so all the specimens used in this investigation were deformed at a temperature of  $360^\circ \text{ C}$ . A three-point bending jig was used, in which the specimen was supported on two quartz knife-edges, whilst its centre was depressed at a constant rate by means of a third quartz knife-edge connected to a motor-driven lead screw. The rate of traverse of the lead screw was chosen so that the glide strain rate in the outermost fibres of the specimen was approximately  $0.8 \times 10^{-5} \text{ sec}^{-1}$ . In each bending experiment a control sample was placed very close to the one being deformed so that the thermal histories of the two were, as near as possible, identical. An atmosphere of forming gas was maintained in the bending apparatus so as to prevent oxidation of the specimens. Since the only components in contact with the specimens were of quartz, the experiments were quite "clean" as regards freedom from impurity contamination.

The load to sustain the imposed deformation rate was measured via the deflection of a calibrated spring; this made the straining jig relatively "soft" with the result that any yield points would not be detected. A typical load vs deflection curve is shown in fig. 3. The feature to which attention is called is the long region of constant load where most of the plastic strain occurred. This behaviour is characteristic of specimens undergoing slip on only one set of planes with no interference from dislocations on other systems [12].

The straining was terminated when the deflection at the centre of the specimen was that required to produce a curvature of  $1/5$  to  $1/6 \text{ cm}^{-1}$ . In a three-point bend test the specimen does not assume a uniform curvature, but rather

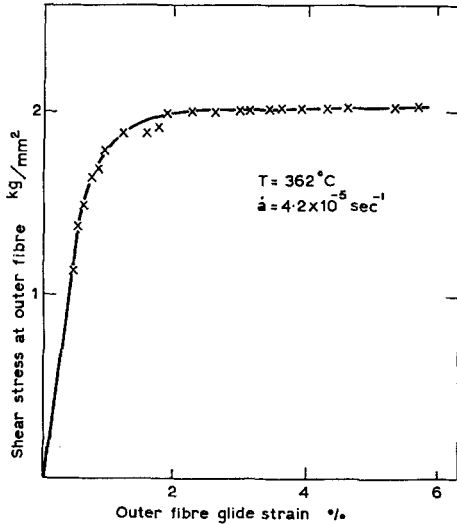


Figure 3 Stress-strain curve obtained in a typical bending experiment ( $\dot{\epsilon}$  is the glide strain rate in the outer fibres of the specimen).

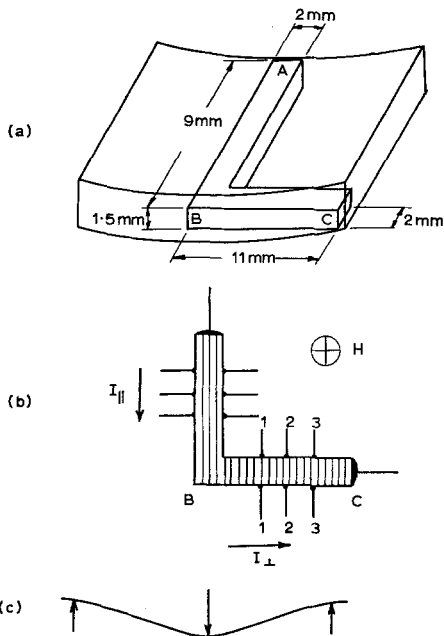


Figure 4 Samples for electrical measurement: (a) origin of the L-shaped specimen in the bent wafer; (b) location of the electrical contacts (shading shows direction of dislocation lines); (c) variation of curvature in a three-point bend test.

takes on the profile in fig. 4 (c), i.e. the radius of curvature varies from a minimum at the inner knife-edges to a maximum at the outer ones. The distribution of dislocations was studied by taking sections of these bent wafers.

Patel [13] has shown that, when silicon samples are bent in the geometry of fig. 2, the dislocation

structure which results consists of long straight dislocations running parallel to the  $\langle 112 \rangle$  bend axis. A similar result would be expected in indium antimonide. Therefore in order to make electrical conductivity and Hall measurements with the current flow first parallel to, and then perpendicular to, the dislocations, L-shaped specimens were cut from the wafers as shown in fig. 4 (a). These were carefully ground by hand until all surfaces were flat, and then the damaged layer was removed by etching. Platinum current leads (0.2 mm diameter) and several pairs of fine platinum potential leads (0.05 mm diameter) were attached with In solder. The potential probes had a contact diameter of about 0.3 mm and a room-temperature resistance of approximately 3 ohms. Control specimens were prepared for measurement in a similar way. The final configuration of an L-shaped specimen prepared for measurement is shown in fig. 4(b). The magnetic field direction is normal to the paper.

Fields of about 1000 gauss were produced by an electromagnet which was calibrated by means of a search coil and fluxmeter. Hall coefficient and conductivity were always measured for at least two values of the current which were of order  $100 \mu\text{A}$  for measurements at  $80^\circ \text{K}$ , and 5 to 10 mA for those at room temperature. At each value, current reversal was carried out, and for the Hall coefficient field reversal also. The differences obtained on reversal were not large – about 10% in the case of Hall voltages and 5% for conductivity measurements. Each specimen was remeasured several times and in most cases independent readings were taken by Latkowski and Willoughby. The maximum error in the Hall coefficients is estimated as  $\pm 12\%$  and in the electrical conductivities as  $\pm 19\%$ .

### 3. Results

#### 3.1. Crystallographic Observations

From a study of the etching characteristics of pairs of samples bent to equal radius but opposite sign of curvature, it was possible to derive: (a) the sign of the curvature; and (b) the number and distribution of both the In- and Sb-dislocations. Consider the specimen of fig. 5(a) which has been bent upwards in the centre. To accommodate the lattice curvature, dislocation half-planes must be introduced from above – in this case these are Sb-dislocations. If they were pure edge dislocations with line direction along the  $\langle 112 \rangle$  bend axis and

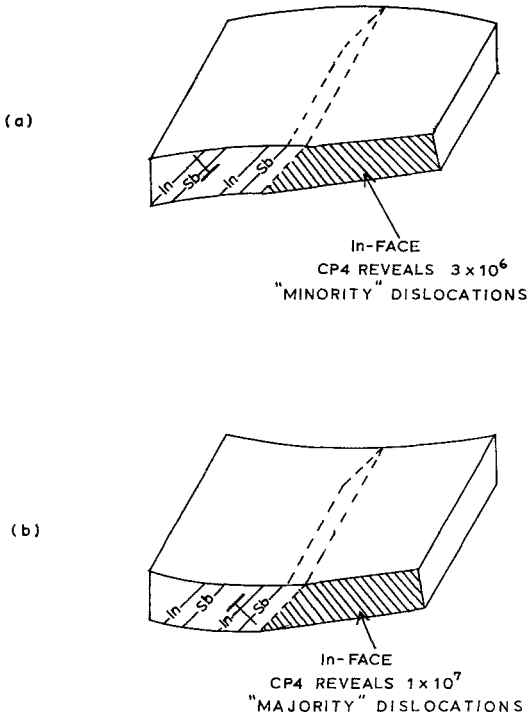


Figure 5 Etching geometry of a pair of bent samples. The etch-pit densities quoted are for specimens bent to a radius of 6 cm. (a) Sb-bending; (b) In-bending.

Burgers vector  $a/2 \langle 110 \rangle$  in the operative slip direction, then the density of dislocations would be

$$\rho_{\text{Sb}} = \frac{1}{r b \cos 45^\circ}$$

where  $r$  is the radius of curvature and  $b = a/2 \langle 110 \rangle$ . Now in any real case plastic deformation will produce dislocations of both signs, but there must always be an excess of the one or the other to maintain the curvature of a bent sample. The situation then becomes

$$\rho_{\text{Sb}} - \rho_{\text{In}} = \frac{1}{r b \cos 45^\circ} \quad (1)$$

The dislocations which are required to maintain the curvature will be termed the "majority" dislocations, and the ones of opposite sign – the "minority" dislocations. In fig. 5(a) the majority dislocations are Sb-type, and in fig. 5(b) – In-type.

In an experiment the first problem is to identify the stacking sequence of the  $\{111\}$  planes, for then the character of the majority dislocations is obtained. By comparing the

intensities of 111 and  $\bar{1}\bar{1}\bar{1}$  X-ray reflections, Warekois [14] was able to show that etch-pits form preferentially on an In rather than on an Sb octahedral face. Thus, if the specimen of fig. 5(a) were sectioned along a  $\{111\}$  slip plane (assumed to be the planes between the widely-spaced layers of atoms), any dislocations threading this cut (say a stray grown-in dislocation) would form a pit on an In face only, and hence enable the polarity of the specimen to be identified.

The actual procedure adopted was a slight modification of this, which enabled both the identification of the sign of the curvature, and the estimation of the number of dislocations introduced by the bending to be obtained in the one step. On account of the  $\bar{4}$  rotation-inversion axes along the  $\langle 100 \rangle$  directions, pairs of identical octahedral faces subtend an angle of  $109^\circ$ , whilst pairs of unlike faces subtend an angle of  $71^\circ$ . Identification of any one face enables the others to be labelled. The  $\{111\}$  section cut was the one making an angle of  $71^\circ$  with the bend axis, so that dislocations running parallel to the latter would intersect the etched face at a steep angle. Typical values obtained with modified CP4\* on two specimens, both bent to a 6 cm radius but in opposite directions, are shown in fig. 5. Both of the counts were made as near as possible to the bend axis, at a point close to the neutral axis. The variation of etch-pit density perpendicular to the neutral plane was only about  $\pm 15\%$  and thus the exact position across the thickness of the sample was not critical.

Now the experiments of Venables and Broudy [16] suggested that In- and Sb-dislocations behave differently in CP4. They concluded that, of the two, only the " $\beta$ "-type formed pits. This work preceded the X-ray identification [14] of the polarity, and since their etching was carried out on  $\{110\}$  planes it is not possible to deduce the identity of their " $\beta$ "-type dislocations. Gatoss *et al* [7] and Holt [6] have predicted on the basis of theoretical models that In-dislocations should be attacked preferentially, but there is no direct experimental evidence on this point. The results of fig. 5 confirm that modified CP4 etches In-dislocations preferentially and suggest that the ratio of the majority to the minority dislocation densities was in this case about 3:1.

More systematic data to support this conclu-

\*1 part HF, 1 part HNO<sub>3</sub>, 2 parts acetic acid.

sion were obtained: (a) by studying the variation of etch-pit density between the inner and outer knife-edge positions; and (b) by re-etching in an inhibited etch which is thought to show up both types of dislocations [15]. This latter treatment will be referred to as the "butylamine etch". The results of a pair of experiments are shown in figs. 6 and 7. Both etches gave pit densities

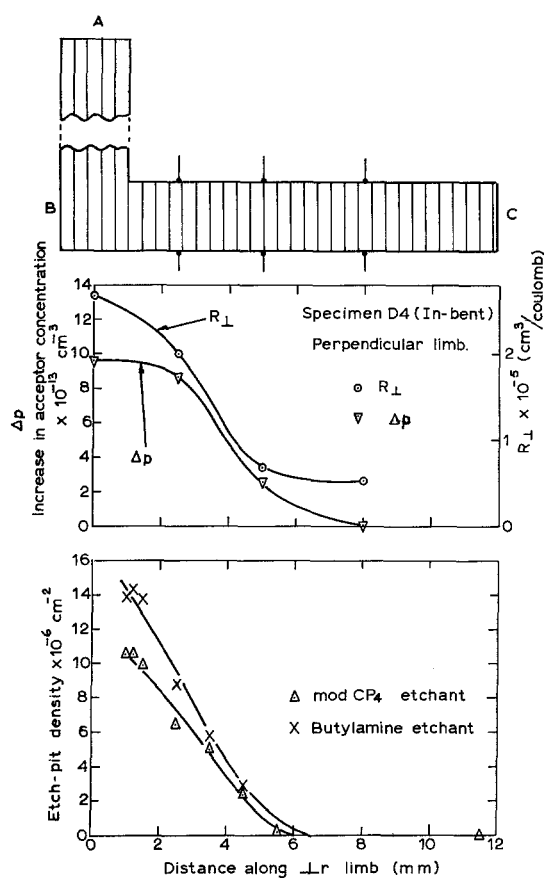


Figure 6 Etch-pit distributions and the variation of the Hall coefficient ( $R_H$ ) along the limb BC of an n-type sample In-bent.

which decreased from a high value, at the position of the centre knife-edge, to values little different from that of the virgin crystal, near the outer knife edges. In the In-bent sample, the etch-pit density with modified CP4 was, at each point, approximately 3/4 of that with the butylamine etch. In the Sb-bent sample, modified CP4 produced about 1/4 the pit density of the inhibited etch. The simplest interpretation of these data is that CP4 etches only In-dislocations whilst the butylamine etch reveals both kinds.

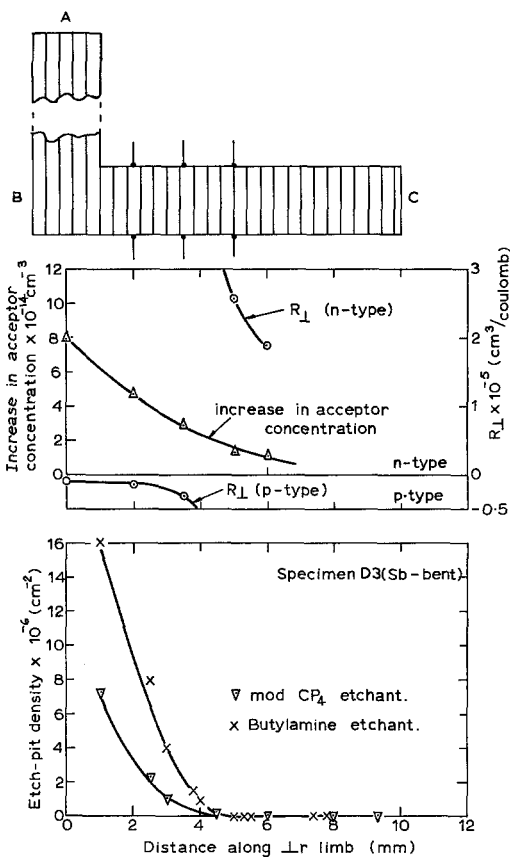


Figure 7 Etch-pit distributions and the variation of the Hall coefficient ( $R_H$ ) along the limb BC of an n-type sample Sb-bent. In this case the number of acceptors introduced was such as to convert the specimen to p-type near the centre.

Thus the In-bent sample contained three times as many In-dislocations as Sb-dislocations, whilst the Sb-bent one had three times as many Sb-dislocations as In-ones. The etch-pit numbers were of the order of magnitude one would expect on the basis of equation 1. However, since the curvature varied continuously from point to point across the sample, it was not possible to test equation 1 rigorously.

The high temperature, low strain conditions chosen for the bending experiments produced a distribution of dislocations which was uniform on a macroscopic scale, but on a microscopic one they were arranged in discrete walls - fig. 8. This polygonised structure might well produce different effects on the electrical properties from an equal density of randomly-distributed dislocations.

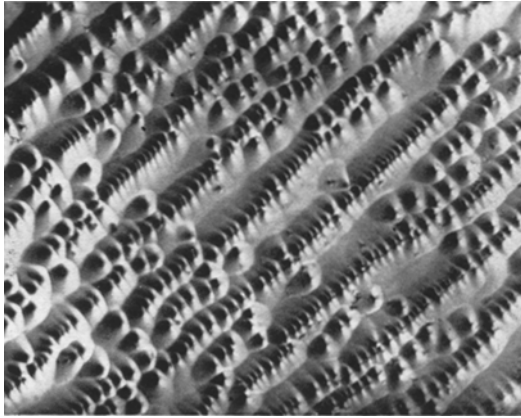


Figure 8 Polygonised array of etch-pits in an In-bent sample, X560.

### 3.2. Conductivity and Hall Coefficient Measurements

#### 3.2.1 Room Temperature Measurements

The electrical conductivity and Hall coefficient measurements on all the deformed samples were equal (to within the estimated experimental error) to the values on the corresponding control samples. All were n-type, with  $[n] =$  the intrinsic number (i.e.  $1.6 \times 10^{16} \text{ cm}^{-3}$ ). It is not surprising therefore that the electron mobilities in the deformed samples were no different from those in the control samples.

#### 3.2.2. Measurements at Liquid-Nitrogen Temperature

(a) *n-type material* Three separate wafers were bent so as to produce a majority of In-dislocations and one bent to produce a majority of Sb-dislocations. In the case of the In-bent

samples electrical measurements were made on an L-shaped specimen cut from one half of each bent wafer, as shown in fig. 4(a). Two L-shaped specimens were prepared from the Sb-bent wafer, one from either side of the bend axis. In all cases the limb AB, cut parallel to the bend axis, was quite uniform, in that Hall voltage and conductivity measurements made at different points along the limb were closely reproducible. The other limb – as would be expected from the etch-pit studies – always showed properties which approximated at the one end (B) to those of the limb AB, and at the other (C) to those of the control specimen.

It is simplest to consider the “parallel” limbs (AB) first. Both directions of bending produced an increase in the concentration of acceptor centres. In the case of those specimens bent Sb-wise this was sufficient to convert the material to p-type at nitrogen temperature.

In table I the Hall coefficient and conductivities are listed for both the control and plastically bent samples, together with the etch-pit densities of the deformed samples (measured as close as possible to the bend axis). Taking the carrier concentrations as  $1/(\text{Hall coefficient} \times \text{electronic charge})$ , the difference between the bent and control samples was assumed to give  $\Delta p$ , the number of acceptors introduced by the deformation. Then using the butylamine etch-pit density the number of acceptors introduced per dislocation site,  $\Delta p.c/\rho_{\text{but}}$  was calculated for each case. These are the values listed in the penultimate column of table I. One striking feature is that for Sb bending the values are approximately four times those for In bending.

TABLE I Samples which were originally n-type. Hall coefficient and conductivity measurements at 80° K. (The subscripts || and c refer to properties measured in the limbs (AB) of deformed samples, and in the “control” samples, respectively)

In-bent samples	$\rho_{\text{CP}_4} (\text{cm}^{-2})$	$\rho_{\text{but.}} (\text{cm}^{-2})$	$R_{  } (\text{cm}^3/\text{C})$	$\sigma_{  } (\text{ohm}^{-1}\text{cm}^{-1})$	$R_c (\text{cm}^3/\text{C})$	$\sigma_c (\text{ohm}^{-1}\text{cm}^{-1})$	$\Delta p.c/\rho_{\text{but.}}$	$\mu_{  }/\mu_c$
D2	$4.9 \times 10^6$	$6.9 \times 10^6$	$5.34 \times 10^5$	0.34	$8.0 \times 10^4$	6.87	0.385	0.332
D5	$8.5 \times 10^6$	$12.5 \times 10^6$	$1.84 \times 10^5$	0.72	$5.43 \times 10^4$	10.5	0.259	0.230
D4	$10.5 \times 10^6$	$14.0 \times 10^6$	$2.75 \times 10^5$	0.64	$5.29 \times 10^4$	10.3	0.273	0.311
Sb-bent samples	$R_{  }$ (p-type)			$R_c$ (n-type)				
D3	$7.3 \times 10^6$	$17.1 \times 10^6$	$8.81 \times 10^3$	0.784	$6.82 \times 10^4$	8.22	1.45	
D3a	$3.5 \times 10^6$	$10.5 \times 10^6$	$1.63 \times 10^4$	0.355	$6.82 \times 10^4$	8.22	1.11	

The last column shows the ratio of the electron mobility in the limb AB to that in the control samples. The changes due to deformation were large, amounting to a reduction of up to  $4 \times$ .

In the "perpendicular" limbs (BC), the Hall coefficient varied along the length. Typical results for an In-bent, and an Sb-bent sample are shown in figs. 6 and 7 respectively. It is seen that changes in carrier concentration are proportional to the local etch-pit density. Because of the fairly rapid variation in carrier concentration along these limbs (BC), it was difficult to obtain the Hall mobility for current flow perpendicular to the dislocations. An approximate value was obtained from the product of the conductivity measured at probes 1 and 3 (fig. 4) and the Hall

In-bending produced large increases in acceptor concentration but no significant change in Hall mobility. Sb-bending produced in the one specimen a small reduction in the acceptor concentration but in the other no measurable change in carrier concentration. However, in both cases there was a significant drop in the Hall mobility. All of these observations were made in the limbs where the current flowed parallel to the dislocations, whose density was estimated by etch-pit counts made as close as possible to the bend axis. These dislocation densities are also listed in table II.

No systematic studies were made of the variation of dislocation density and electrical properties in the limbs (BC) in these samples.

TABLE II Samples which were originally p-type. Electrical measurements at  $80^\circ$  K. (The subscripts || and c refer to properties measured in the limbs (AB) of deformed samples, and in the "control" samples, respectively)

In-bent samples	$\rho_{CP4}$ ( $\text{cm}^{-2}$ )	$\rho_{\text{but.}}$ ( $\text{cm}^{-2}$ )	$R_{  }$ ( $\text{cm}^2/\text{C}$ )	$\sigma_{  }$ ( $\text{ohm}^{-1}\text{cm}^{-1}$ )	$R_c$ ( $\text{cm}^2/\text{C}$ )	$\sigma_c$ ( $\text{ohm}^{-1}\text{cm}^{-1}$ )	$\Delta p.c/\rho_{\text{but.}}$	$\mu_{  }/\mu_c$
A1	$1.93 \times 10^6$	$2.3 \times 10^6$	$6.58 \times 10^3$	1.28	$9.25 \times 10^3$	0.761	4.93	1.20
A2	$3.9 \times 10^6$	$4.9 \times 10^6$	$5.85 \times 10^3$	0.99	$1.45 \times 10^4$	0.582	5.18	0.684
Sb-bent samples								
A4	$6.15 \times 10^6$	$16.4 \times 10^6$	$1.62 \times 10^4$	0.41	$1.22 \times 10^4$	0.85	0.305	0.650
A5	$4.8 \times 10^6$	$8.2 \times 10^6$	$1.17 \times 10^4$	0.50	$1.17 \times 10^4$	0.80	0	0.619

coefficient at probes 2-2. In the In-bent specimens, the Hall mobilities calculated in this way were less than  $1.0 \times 10^5 \text{ cm}^2 \text{ V}^{-1} \text{ sec}^{-1}$ , i.e. at least a factor of 2 less than the mobility with current flow parallel to the dislocations, and a factor of about 8 less than the mobility in the control specimens. The Sb-bent samples, which were converted to p-type on bending, showed an anisotropy in the hole mobility of about a factor of 2.

(b) *p-type material* Two separate wafers were bent to produce an excess of In-dislocations and two to produce an excess of Sb-dislocations. For electrical measurements an L-shaped specimen was cut from each. The properties in the limbs (AB), where the current flow was parallel to the dislocations, were again found to be quite uniform along the length of these limbs. Table II gives detailed information similar to that given in table I, which was described in the previous section.

## 4. Discussion

### 4.1. The Dislocation Structure as Revealed by Etching

The etching experiments described in this paper confirm the conclusion of Venables and Broudy [16] that, in indium antimonide, dislocations of the one sign etch more rapidly than those of the opposite sign. It is shown unambiguously for the first time, that modified CP4 attacks indium dislocations preferentially, whilst the butylamine etch reveals both In- and Sb-dislocations equally. This is the behaviour predicted by Gatos and Lavine [7]. Because three-point bending does not produce a uniform curvature it was not possible to make a quantitative check of the etching behaviour via equation 1. However, one of us, Willoughby [17], has recently carried out a series of four-point bending and annealing experiments which permit assessment of the action of these etches. These results

confirm that butylamine etch shows up both the In- and the Sb-dislocations, but that modified CP4 etch attacks not only all the In-dislocations but also a fraction – probably about half – of the Sb-ones. In view of these results the majority: minority ratios deduced in section 3.1 require slight adjustment, but certainly give the correct order of magnitude.

The fact, that the bent samples all contained about one third as many dislocations of the sign opposite to that required to maintain the lattice curvature as compared with the number of those of the correct sign, will have to be borne in mind when considering the electrical effects. Here it is worth discussing the dislocation dynamics which might give rise to such a small majority:minority ratio. It is interesting to contrast the present results with those of Livingston [18] on copper. (This is the only other case where an etch which can discriminate between dislocations of opposite sign has been developed.) He found that, in copper crystals bent at room temperature, about 95% of the dislocations were of the majority sign. This result was explained in terms of the dominant role of surface sources – only majority sign dislocations move towards the neutral axis under a bending stress. To account for the present results on indium antimonide where there were relatively large numbers of minority dislocations, it is necessary to invoke internal sources of some kind. Since the total dislocation density in the virgin crystals was only of order  $10^3 \text{ cm}^{-2}$ , it seems unlikely that the minority sign dislocations issued from internal Frank-Read sources. It also seems doubtful whether the double cross-glide multiplication mechanism is an important one in the diamond and sphalerite structure materials. The phenomenon of slip-band broadening, which was first seen in lithium fluoride and discussed by Johnston and Gilman [19] in terms of propagation by double cross-glide, does not occur in germanium or silicon. On the other hand Holt and Crawford (private communication) have observed elementary structure in the slip-line pattern of germanium; this is sometimes taken as evidence for double cross-slip. Dew-Hughes [20] first suggested that the absence of cross-slip in germanium might account for some of the differences between its behaviour and that of lithium fluoride. Subsequently Alexander and Haasen [21] found evidence for the deviation of slip lines by the climb of edge dislocations but not by the cross-slip of screws. If the propagation

of slip along a virgin specimen were dependent on the climb of edge segments this would account for the temperature sensitive yielding behaviour of these materials.

#### 4.2. The Electrical Effects of Dislocations

The effects of deformation by bending on the carrier concentration may be summarised as: (a) *In-bending* introduced acceptor centres into both p- and n-type materials; (b) *Sb-bending* introduced acceptors into material originally n-type. However, specimens which were originally p-type showed no increase in acceptor concentration; in fact, in one case there was a small decrease – i.e., an introduction of donor centres.

##### 4.2.1. A Possible Energy Level Scheme

All of the above results can be accounted for qualitatively if one assumes that the energy levels of the centres associated with the dislocations are in the approximate positions shown in fig. 9. The low-lying acceptor level of the In-

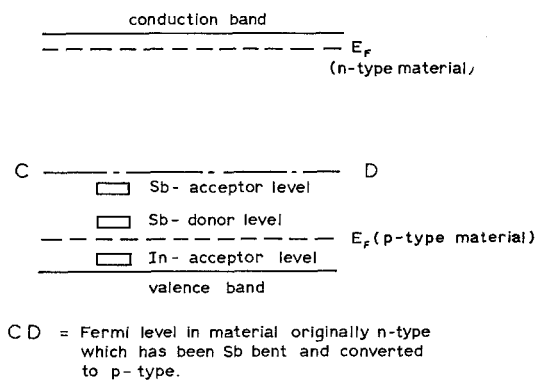


Figure 9 Scheme of energy levels for the dislocation centres.

dislocation would be ionised in both n- and p-type materials. The dual role of the Sb-dislocations is ascribed to a high acceptor level and a low-lying donor level. Thus, in n-type material Sb-acceptor centres would be ionised but not the Sb-donor centres, and the final position of the Fermi level would be either above or below the middle of the gap depending on the number of dislocations introduced. In material originally p-type the Sb-donors would be ionised but not the Sb-acceptors.

The dislocation energy levels suggested in fig. 9 agree with some but not all of the previously published results. However, it is con-



venient to defer consideration of these discrepancies until later.

#### 4.2.2. *n*-type Material In-bent

This is the most straightforward of the four cases to consider. The results clearly indicate an acceptor action, which agrees with the previous findings of Gatos *et al* [9] and with the predictions of both Gatos *et al* [7] and Holt [6]. The theory of Read [22] can be adapted in order to make quantitative comparisons with experiment.

On the Shockley-Read model a dislocation in the diamond structure has unpaired electrons spaced at a distance  $c$  along its core, where  $c$  is related to  $b$ , the Burgers vector of the dislocation, and  $\alpha$ , the angle between the dislocation line direction and its Burgers vector, by the equation:

$$c = 0.866 b \operatorname{cosec} \alpha$$

Gatos and Lavine [7] and Holt [6] have modified the model for the case of the Sphalerite structure, but the important point is that neither of the two kinds of dislocation in this structure has more than  $1\frac{1}{3}$  "sites" per atom length along the dislocation. Moreover, as Read has shown, the coulombic repulsion between neighbouring ions results in the dislocation sites being only partially occupied at all temperatures. Adapting the formulae given by Read, it is found that the maximum possible value of  $f$ , the fraction of sites occupied, for dislocation acceptor centres in InSb is 0.12. This occurs at  $T = 0^\circ \text{K}$  with the Fermi- and acceptor-levels set at the top and bottom of the band gap, respectively. With the levels in these same positions  $f$  falls to about 0.1 at  $80^\circ \text{K}$ , and to lesser values for smaller separations of the Fermi- and acceptor-levels. These values are to be compared with those deduced from experiment which are listed under  $\Delta p.c/\rho_{\text{but}}$  in table I. The butylamine etch is believed to reveal both the In- and the Sb-dislocations, but still the numbers of acceptors introduced per dislocation site are a factor of 3 too large. Such a discrepancy is not far outside our limits of confidence on the dislocation density, but before discussing this point it is interesting to consider the mobility results.

Firstly, the electron mobility for current flow parallel to the dislocations should be unchanged on Read's specular reflection model. In fact it was found that  $\mu_{\parallel}/\mu_c = (0.23 \text{ to } 0.33)$ . Such an effect could be ascribed to dislocations

running transverse to the bend axis, but great care was taken to avoid this.

Secondly, the mobility measured perpendicular to the dislocations,  $\mu_{\perp}$ , may be examined. Logan, Pearson and Kleinman [23] developed Read's treatment and obtained,

$$\frac{\mu_{\perp}}{\mu_c} = g(\epsilon) \cdot F(X) \quad (2)$$

where  $g(\epsilon)$ , the "distortion effect" arises from the distortion of the current streamlines around the insulating space charge tubes whose fractional volume is  $\epsilon$ , and  $F(X)$  the "scattering effect" is due to specular reflection of carriers from the surface of the dislocation tubes. The function  $g(\epsilon)$  was obtained empirically by Read [22] and has since been calculated by Juretschke [24]. In the scattering function  $X = l/l_D$ , where  $l$  is the mean free path of electrons in normal material and  $l_D$  that in deformed. Assuming the mobility to be limited by acoustic scattering,  $l$  is given by the classical expression derived by Wilson [25]. Logan *et al* [23] obtained  $l_D = 3/(8R_s\rho)$ , where  $R_s$ , the radius of the space charge tubes, was given by Read [22], as

$$R_s = \left[ \frac{f}{\pi c (N_d - N_a)} \right]^{\frac{1}{2}}$$

Logan *et al* [23] have given a graph of  $F(X)$  as a function of  $X$ . Substituting in these various relations from the data for specimen D5 in table I, and assuming the dislocation density to be equal to the butylamine etch-pit density, and  $f = 0.1$ , we obtain  $R_s = 8.32 \times 10^{-5} \text{ cm}$ ,  $l_D = 3.61 \times 10^{-4} \text{ cm}$  and  $l = 2.38 \times 10^{-4} \text{ cm}$ .

These values give  $F(X) = 0.63$ ,  $\epsilon = \frac{\rho}{c} \frac{f}{N_d - N_a} =$

0.272, and  $g(\epsilon) = 0.78$ . Substituting in equation 2

$$\frac{\mu_{\perp}}{\mu_c} = 0.63 \times 0.78 = 0.491$$

but, by experiment,  $\frac{R_{\perp} \sigma_{\perp}}{R_c \sigma_c} = 0.17$

This is a very large discrepancy, but the agreement is improved if the dislocation density is taken as three times the etch-pit density, when  $g(\epsilon) = 0.5$ ,  $F(X) = 0.37$  and  $\mu_{\perp}/\mu_c = 0.18$ .

To conclude, the changes in both the carrier concentration and in the electron mobility perpendicular to the dislocations can be accommodated by the Read theory if one adjusts the measured dislocation density by a factor of

three, and assumes the maximum separation of Fermi- and dislocation-acceptor levels. The big changes in electron mobility parallel to the dislocations are not explained.

These limitations can be avoided by adopting the postulate suggested by Broudy [4] that the reflection of electrons at the dislocation tubes is non-specular. On this model the material becomes divided into a system of two sets of parallel conductors with a set of parallel insulating cores – the dislocation space charge tubes. The interpretation of the conductivity and Hall coefficient measurements is no longer straightforward. For two uniform parallel conductors of conductivities  $\sigma_1$  and  $\sigma_2$ , carrier concentrations  $n_1$  and  $n_2$ , electron mobilities  $\mu_1$  and  $\mu_2$ , the Hall coefficient and conductivity of the composite, when the current flows parallel to the interface and the magnetic field perpendicular to it, are given by

$$R = \frac{(1 + \beta)(1 + \beta\mu_1\sigma_1/\mu_2\sigma_2)}{n_2e(1 + \beta\sigma_1/\sigma_2)^2} \quad (3)$$

$$\text{and} \quad \sigma = (\sigma_2 + \beta\sigma_1)/(1 + \beta) \quad (4)$$

where  $\beta$  is the ratio of the cross-sectional areas of conductors 1 and 2. Applying these relations to the case of n-type material containing dislocations, Broudy identified region 2 with a cylindrical shell of thickness equal to one mean free path, within which the electron mobility is reduced by non-specular reflections to a value  $\mu_2$ , which is less than  $\mu_1$ , the mobility in the regions further away from the dislocations. Thus the fraction of material in the cylindrical shells is

$$\phi = \rho\pi(l^2 + 2R_s l),$$

and in the  $\mu_1$ -regions  $(1 - \epsilon - \phi)$ , where  $\epsilon$  is the quantity used in the Read treatment. Using equations 3 and 4 he obtains

$$R_{\parallel}/R_c = \frac{1 - \epsilon - (1 - \theta^2)\phi}{[1 - \epsilon - (1 - \theta)\phi]^2} \quad (5)$$

$$\text{and} \quad \sigma_{\parallel}/\sigma_c = 1 - \epsilon - (1 - \theta)\phi \quad (6)$$

where  $\theta = \mu_2/\mu_1$ , and the suffices  $\parallel$  and c refer to properties measured parallel to the dislocations, and in an undeformed specimen, respectively. All of the quantities in these formulae except  $\theta$  are calculable.  $\theta$  has to be treated as an adjustable parameter. In the case of indium antimonide the estimation of  $\phi$  is complicated by the fact that  $l$  is long and the  $\phi$ -regions tend to overlap. Thus, in the present case, where the dislocations were polygonised, the arrange-

ment of the  $\epsilon$ -, and  $\phi$ -regions is pictured as in fig. 10. From this figure  $\phi$  is estimated as approx-

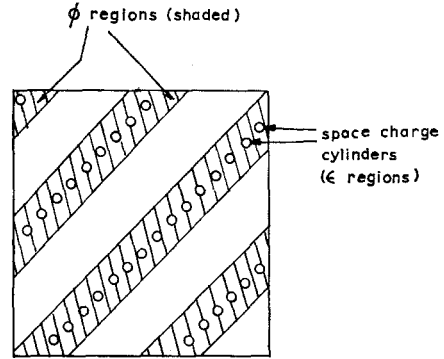


Figure 10 Modified Broudy model for samples with polygonised dislocations.

imately 0.7. With  $\epsilon = 0.272$ , as obtained earlier, and  $\theta = 0.1$

$$R_{\parallel}/R_c = 3.645 \text{ and } \sigma_{\parallel}/\sigma_c = 0.098$$

compared with the experimental values of 3.4 and 0.07, respectively. The agreement here is much better than that afforded by the values predicted on the Read theory: 1.37 and 0.728, respectively.

The results of previous work on InSb are listed in table III. Values of  $\Delta p.c/\rho$  (or  $\Delta n.c/\rho$ ) had to be calculated by substituting the value of  $\rho$  predicted from the bend radius by equation 1, as in none of these experiments was the etch-pit technique used. One would expect this procedure to underestimate the real dislocation density by up to a factor of five, but this is insufficient to account for even the smallest value of  $\Delta p.c/\rho$  which is  $30\times$  the maximum value predicted on the Read theory. The In-bent n-type specimens of Gatos *et al* [9] showed particularly large acceptor effects in quite heavily-doped starting material. Thus, in table III  $\Delta p.c/\rho$  for their specimens has a value which is a factor of at least 100 greater than that predicted on the straightforward Read theory. The Broudy modification does not cope with this result either, for  $R_s$  and  $l$  are small at such doping levels, with the result that  $\epsilon$  and  $\phi$  are both of order  $10^{-2}$  or less, and equations 5 and 6 would predict extremely small effects on the Hall coefficient and conductivity.

#### 4.2.3. p-type Material In-bent

It is convenient to treat this case next although there is no previous work with which to com-

TABLE III Summary of previous work on InSb. All measurements relate to 77° K

Author	Type of deformation	Radius of bend	$n_c$	$n_d$	$\mu_c$	$\mu_d$	$\frac{(\Delta n \text{ or } \Delta p) \times c}{\rho}$
Gatos <i>et al</i> [9]	Double slip, 300° C In-bent	15 cm	$1.5 \times 10^{15}$	$8.2 \times 10^{14}$	$2.2 \times 10^5$	$8.6 \times 10^4$	10.7
Gatos <i>et al</i> [9]	As above but Sb-bent	8 cm	$3.9 \times 10^{15}$	$1.0 \times 10^{16}$	$1.7 \times 10^5$	$5.6 \times 10^4$	51.2*
Duga [8]	Multiple Slip, majority dislocation not identified	200 cm	$4.8 \times 10^{14}$	$2.5 \times 10^{14}$	$2.6 \times 10^5$	$1.8 \times 10^5$	44.2
Duga [8]	Multiple Slip majority dislocation not identified	15 cm	$2.6 \times 10^{15}$	$1.04 \times 10^{15}$	$2.2 \times 10^5$	$9.3 \times 10^4$	24.4
Broudy [4]	Double slip, 305° C majority dislocation not identified	25 cm	$6.9 \times 10^{14}$	$5.7 \times 10^{14}$	$3.6 \times 10^5$	$2.0 \times 10^5$	3.3

\*This relates to donor action. All others to acceptor action.

pare present results. In Ge, early work suggested that there was no dislocation acceptor action in p-type material, and it was concluded that the acceptor level active in n-type material must reside in the upper half of the gap. More recently, Blik [26] has found acceptor action in p-type germanium and he has begun to work out a theory for this case. He considers the negatively-charged dislocations to be screened by a high local concentration of free holes. The statistics of the occupation of the dislocation acceptor centres are worked out using the screening length,  $\lambda$ , as a free parameter. Comparison with experiment leads to a value of  $\lambda$  of about 10 atomic spacings. This is very much smaller than one would expect, for substituting  $p = 10^{14} \text{ cm}^{-3}$ ,  $\kappa = 16$  and  $T = 77^\circ \text{ K}$  in the expression  $1/\lambda^2 = 4\pi e^2 p / \kappa k T$ , due to Brooks [27],  $\lambda$  is obtained as  $2.5 \times 10^{-5} \text{ cm}$ .

An apparent shortcoming of the Blik treatment is the assumption that the free holes surrounding the dislocations contribute to  $R$  in just the same way as the holes remote from the dislocations, or, to put it another way, that the number of acceptors,  $\Delta p$ , introduced by the deformation is simply given by

$$\Delta p = \frac{1}{e} \left( \frac{1}{R_d} - \frac{1}{R_c} \right) \quad (7)$$

where  $R_c$  and  $R_d$  are the Hall coefficients in the control and deformed samples. Now it is clear that the diameter of the  $p^+$  regions around the dislocations must be of the same order as  $\lambda$ , so that with  $f \sim 0.1$ , the hole concentration near

the dislocations will be of order  $5 \times 10^{18} \text{ cm}^{-3}$  for  $\lambda = 4 \times 10^{-7} \text{ cm}$ , and  $1.3 \times 10^{15} \text{ cm}^{-3}$  for  $\lambda = 2.5 \times 10^{-5} \text{ cm}$ . In either case the conductivity of the  $p^+$  regions is likely to be significantly different from that in the surrounding medium and the Hall coefficient will not have the simple physical significance it has in a homogeneous material.

It seems appropriate, therefore, to interpret these data in terms of the two region equations 3 and 4. The material is pictured as two sets of parallel conductors—a  $p^+$  region around the dislocations with a carrier mobility somewhat less than that in the other region remote from the dislocations. If one makes the simplifying assumption that the mobility in the  $p^+$  regions is no different from that in the surrounding regions, which in turn may be equated to  $\mu_c$ , equation 3 reduced to the simple equation 7 and the two-region analysis makes no difference to the outcome of the interpretation.

Now, theoretical calculations of  $f$  by the method of Blik result in values of less than 0.1 at  $80^\circ \text{ K}$ , even using an artificially low screening length. Thus, the abnormally high values of  $\Delta p.c/\rho$  listed in table II cannot be explained satisfactorily in terms of the dangling-bond model, since one would need to assume that the etch-pit techniques underestimated the dislocation density by a factor of 50. Furthermore, a Broudy-type model, involving a third region within which the mobility is reduced by non-specular scattering at  $p^+$  cylinders, could not help to explain the results, since the mean

free path of holes in indium antimonide is very small ( $\sim 10^{-5}$  cm) and this third region would have little influence on properties measured parallel to the dislocations.

#### 4.2.4. n-type Material Sb-bent

Here the present results are at variance with the donor action reported by Gatos *et al* [9]. The behaviour he reported is very difficult to understand. That it should be necessary to start off with a material containing not less than  $10^{15}$  donors per  $\text{cm}^3$ , i.e. with a high Fermi level, in order to observe a donor action seems the wrong way about. The fact that  $\Delta n.c/\rho$  should be greater than 1 (see table III) is perhaps an indication that the observed action was not due to dislocations. If it were due to dislocations, a model similar to that outlined in the last section, but with the dislocation donors screened by free electrons, would be needed.

Whilst the presently observed acceptor action of Sb-dislocations in n-type material is more easily understood, the higher values of  $\Delta p.c/\rho_{\text{but}}$  (c.f. those for In-bending) do not accord with the relative positions of the Sb- and In-levels deduced in section 4.2.1. Nor does recourse to a Broudy two-region model help. This problem remains unsolved at the present time.

#### 4.2.5. p-type Material Sb-bent

There are no previous results for this case, and the present ones are not such as to justify a detailed analysis. The appropriate model appears to be the converse of the Read case – positively-charged dislocation donor sites screened by (static) tubes of ionised acceptor atoms. The  $\Delta p.c./\rho_{\text{but}}$  values seem reasonable, and this would appear to be a straightforward case.

#### 4.2.6. Possible Role of Point Defects and Impurities

The possibility that the effects described above were due to point defects or impurities has to be considered. Other possibilities such as jogged dislocations and Shockley's [28] dislocation "edge-states" have been considered and ruled out. In the present experiments the deformation geometry and conditions were chosen so as to minimise point-defect production. Furthermore, Willoughby [17] reports that a heat treatment, closely similar to that used in the present experiments, caused no changes in either undeformed or in previously deformed specimens. It seems, therefore, that neither point

defects nor impurities alone could have been responsible for the observed electrical changes. The anisotropic nature of the deformed samples gives further support to this contention, but leaves the possibility that impurities were dragged into the material by the gliding dislocations [29].

## 5. Summary and Conclusions

The present results confirm previous findings that In- and Sb-dislocations have different etching behaviour, and that In-dislocations are revealed preferentially by certain etchants. In samples bent at  $360^\circ\text{C}$ , where dislocation annihilation should be easy, it was found that the density of the majority sign dislocations was only about three times that of the minority sign ones. Reasons for this behaviour were discussed.

The electrical behaviour of samples bent in opposite directions clearly revealed that different kinds of centres had been introduced into the forbidden gap. The behaviour was not as straightforward as that predicted by the simple theory of Gatos *et al* [7], for whilst In-bending introduced acceptors into both p- and n-type materials, Sb-bending introduced large numbers of acceptors into n- and small numbers of donors into p-type material.

The detailed reasoning of section 4.2.6 leaves little doubt as to the importance of the dislocations in producing these effects. However, the effects observed in two of the four cases studied were at least an order of magnitude too large to be accounted for on present theories. It has been shown in table III that previous work gave even larger discrepancies with these theories. This points to the need either to invoke a dislocation-impurity interaction, or for a new theory of dislocation action in indium antimonide.

## Acknowledgements

The authors are indebted to Professor J. G. Ball for provision of laboratory facilities. Financial support was provided by the Scientific Research Council, the Admiralty, and the Trustees of the Beit Fellowship for Scientific Research. Grateful thanks are extended to these bodies and also to Drs J. B. Mullin, K. F. Hulme, and colleagues at RRE, Malvern, who supplied the crystals, and also took part in many useful discussions. The paper is published by permission of the Controller, HM Stationery Office.

## References

1. P. HAASEN and A. SEEGER, *Halbleiterprobleme (Braunschweig: Vieweg)* **4** (1958) 68.
2. W. BARDSLEY, *Progr. in Semiconductors* **4** (1959) 157.
3. VAN BUEREN, "Imperfections in Crystals" (North Holland Publishing Co, 1960).
4. R. M. BROUDY, *Advances in Physics* **12** (1963) 135.
5. P. HAASEN, *Acta. Met.* **5** (1957) 598.
6. D. B. HOLT, *J. Phys. Chem. Solids* **23** (1962) 1353.
7. H. C. GATOS and M. C. LAVINE, *J. Electrochem. Soc.* **107** (1960) 427.
8. J. J. DUGA, *J. Appl. Phys.* **33** (1962) 169.
9. H. C. GATOS, M. C. FINN and M. C. LAVINE, *J. Appl. Phys.* **32** (1961) 1174.
10. R. K. MUELLER and R. L. JACOBSEN, *J. Appl. Phys.* **33** (1962) 2341.
11. J. CZOCHRALSKI, *Z. Phys. Chem.* **92** (1917) 219.
12. R. L. BELL and W. BONFIELD, *Phil. Mag.* **9** (1964) 9.
13. J. R. PATEL, *J. Appl. Phys.* **29** (1958) 170.
14. E. P. WAREKOIS, *Lincoln Lab. Quarterly Progress Report* (15 July 1959) 45.
15. H. C. GATOS and M. C. LAVINE, *J. Appl. Phys.* **31** (1960) 743.
16. J. D. VENABLES and R. M. BROUDY, *J. Appl. Phys.* **29** (1958) 1025.
17. A. F. W. WILLOUGHBY, Ph.D. Thesis (London) (1965).
18. J. D. LIVINGSTON, "Direct Observations of Imperfections in Crystals" (Interscience, 1962), p 115.
19. W. G. JOHNSTON and J. J. GILMAN, *J. Appl. Phys.* **31** (1960) 632.
20. D. DEW-HUGHES, *IBM J. Res. Dev.* **5** (1961) 279.
21. H. ALEXANDER and P. HAASEN, *Acta Met.* **9** (1961) 1001.
22. W. T. READ, *Phil. Mag.* **45** (1954) 775; *ibid* **45** (1954) 1119; *ibid* **46** (1955) 111.
23. R. A. LOGAN, G. L. PEARSON and D. A. KLEINMAN, *J. Appl. Phys.* **30** (1959) 885.
24. H. J. JURETSCHKE, R. LANDAUER and J. A. SWANSON, *J. Appl. Phys.* **27** (1956) 838.
25. A. H. WILSON, "The Theory of Metals" (Cambridge University Press, 1958).
26. L. BLIEK, Dipl. Thesis (Göttingen) (1964).
27. H. BROOKS, *Adv. in Electronics and Electron Physics* **7** (1955) 156.
28. W. SHOCKLEY, *Phys. Rev.* **91** (1953) 228.
29. A. H. COTTRELL and M. A. JASWON, *Proc. Roy. Soc. A* **199** (1949) 104.